JOURNAL OF THERMOPHYSICS AND HEAT TRANSFER
Vol. 20, No. 3, July–September 2006

Coupled Rotational–Vibrational Relaxation of Molecular Hydrogen at High Temperatures

Michiko Furudate,* Kazuhisa Fujita,† and Takashi Abe‡
Institute of Space and Astronautical Science, Sagamihara 229-8510, Japan

The internal energy relaxation processes of molecular hydrogen in the temperature range of 1000–50,000 K are investigated by integrating the master equation considering all of the rotational and the vibrational energy levels simultaneously. The state-to-state and the state-specific dissociation rate coefficients used in the calculation are determined by a quasi-classical-trajectory analysis. The obtained rates are validated against the existing experimental data. Recombination rate coefficients for bulk gas are also calculated from the detailed rates and compared with the existing studies. From the calculated evolutions of energies in the rotational and the vibrational modes, the relaxation times of these two modes for the Landau–Teller equation are derived. The obtained relaxation times agree fairly well with the existing experimental data for the temperatures up to 1000 K for the rotational relaxation and up to 3000 K for the vibrational relaxation. It was revealed that these two energy modes are strongly coupled at high temperatures. The effective collision numbers required for equilibration of the two modes are found to vary from 6 to 600. The approximate expressions describing energy relaxation of the coupled ro–vibrational mode are derived for temperatures from 5000 to 50,000 K.

Nomenclature

b	=	impact parameter, m
E_{rv}	=	ro–vibrational energy, J
$e_{J,v}$	=	ro–vibrational energy of state (J, v), J
e_{rot}	=	average rotational energy per molecule, J
$e_{\mathrm{rot-vib}}$	=	average ro–vibrational energy per molecule, J
e_{vib}	=	average vibrational energy per molecule, J
J	=	rotational quantum number
K_c	=	elastic collision rate
$K_{c\to J,v}$	=	normalized state-specific recombination rate coefficient
K_{eq}	=	equilibrium constant, m^{-3}
$K_{J,v\to c}$	=	normalized state-specific dissociation rate coefficient
$K_{J,v\to J',v'}$	=	normalized state-to-state transition rate coefficient
k	=	Boltzmann constant, 1.3806×10^{-23} J/K
$k_{c\to J,v}$	=	state-specific recombination rate coefficient, m^6/s
k_d	=	dissociation rate coefficient in the bulk gas, $\mathrm{m}^3/\mathrm{s}^2$
$k_{J,v\to c}$	=	state-specific dissociation rate coefficient, m^3/s
$k_{J,v\to J',v'}$	=	state-to-state transition rate coefficient, m^3/s
k_r	=	recombination rate coefficient in the bulk gas, m^6/s
m	=	molecular weight, kg
$N_{J,v\to J',v'}$	=	number of event $J, v \to J', v'$
N_{trial}	=	total number of trial trajectory calculation
n_{H}	=	number density of atomic hydrogen, m^{-3}
$n_{\mathrm{H_2}}$	=	number density of molecular hydrogen, m^{-3}
$n_{J,v}$	=	number density of molecular hydrogen in the state (J, v), m^{-3}
P	=	probability
p	=	pressure, atm
T	=	translational temperature, K
T_r	=	bulk rotational temperature, K
T_v	=	bulk vibrational temperature, K
t	=	time, s
t_c	=	mean collision time, s
U	=	random number between 0 and 1
Z	=	collision number
γ_J	=	line-broadening coefficient, $\mathrm{cm}^{-1}\ \mathrm{atm}^{-1}$
θ_v	=	characteristic vibrational temperature, K
μ	=	reduced mass, kg
ρ_{H}	=	normalized nonequilibrium population of atomic hydrogen
$\rho_{J,v}$	=	normalized nonequilibrium population in the state (J, v)
τ	=	ro–vibrational relaxation time, s
τ_r	=	rotational relaxation time, s
τ_v	=	vibrational relaxation time, s
Ω	=	collision integral

Subscripts

eq	=	equilibrium
0	=	initial state

Presented as Paper 2003-3780 at the AIAA 36th Thermophysics Conference, Orlando, FL, 23–26 June 2003; received 28 February 2005; revision received 2 August 2005; accepted for publication 2 August 2005.

*JSPS Research Fellow, Department of Space Transportation Engineering; currently BK21 Research Fellow, Department of Mechanical and Aerospace Engineering, Seoul National University, Shilim-Dong, Gwanak-Gu, Seoul, 151-742 Republic of Korea; furu@snu.ac.kr. Member AIAA.

†Research Associate, Department of Space Transportation Engineering; currently Senior Researcher, Aerodynamics Research Group, Institute of Space Technology and Aeronautics, Japan Aerospace Exploration Agency, 7-44-1 Jindaijihigashimachi, Chofu, 182-8522 Japan; kazu@kazudom.com. Senior Member AIAA.

‡Professor, Department of Space Transportation Engineering, Yoshinodai 3-1-1; tabe@gd.isas.jaxa.jp. Associate Fellow AIAA.

I. Introduction

TO design a proper thermal protection system of an entry probe for a planetary mission, it is necessary to estimate accurately the amount of heat flux to the probe's surface. In 1995, Galileo probe entered into the Jovian atmosphere with a relative velocity of 47.4 km/s. The observed surface recession profile of the ablative heatshield during the entry flight was significantly different from those of the preflight calculations.[1] The recession of the ablation material was approximately one-half in the stagnation region and twice over the frustum in the downstream region compared with the predictions. Postflight investigations revealed that the flight data over the frustum are most likely caused by an earlier transition from the laminar into the turbulent boundary layer, which is induced by injection of gas from the surface due to ablation.[2,3] On the other hand, the problem in the stagnation region is left unsolved. In general, the atmosphere of all outer planets consists mostly of hydrogen and helium. For future outer planetary missions, it is necessary to

explain completely the causes of the discrepancy between the flight data and the preflight calculations.

A failure to predict the recession rate in the stagnation region in the preflight calculations may be attributed to exclusion of describing nonequilibrium phenomena.[2] Before the Galileo mission, Leibowitz conducted an emission measurement in a hydrogen–helium mixture in a shock tube to examine the ionization process behind shock wave.[4] According to the experiment, the ionization process of atomic hydrogen has a finite incubation period behind the shock wave. Howe derived a formula from Leibowitz's data that gives the time to reach the peak degree of ionization behind a shock wave.[5] The study indicated that the un-ionized region would be as large as one-half of the shock layer thickness in the maximum heating conditions along Galileo probe's entry trajectory, in which the stagnation pressure was of the order of 10 atm; the ionization nonequilibrium phenomenon is prominent despite the high pressure. In the Galileo probe's entry flight, the dominant heat transfer was contributed by radiation from ionized hydrogen. The nonequilibrium makes the ionized region thinner, resulting in a smaller radiative heat flux reaching the wall than that in an equilibrium flow.

In the flows consisting of hydrogen and helium under consideration, electrons are first produced by photoionization ahead of the strong shock wave,[6] whereas molecular hydrogen is dissociated behind the shock wave. Atomic hydrogen is then ionized mainly due to electron-impact ionization, resulting in a rapid increase in electron number density, which is so-called the avalanche ionization.[7] In such processes, flows immediately behind the shock wave are slightly ionized but are mostly undissociated. Electron temperature, which has a significant influence on initiation of the avalanche ionization, is considered to be dictated by interaction with internal modes of hydrogen molecules through inelastic collisions.[8] Therefore, it is important to examine the relaxation processes of the internal energy modes of molecular hydrogen.

In the cases of nitrogen and oxygen molecules, the rotational relaxation completes quickly compared with the vibrational relaxation. Therefore, an assumption of equilibrium between translational and rotational energy modes is acceptable in general in numerical simulations of entry flows into Earth's atmosphere. Only the vibrational energy mode is assumed to be in nonequilibrium with the translational mode.[9] However, for hydrogen flows, these assumptions fail because the rotational relaxation time for molecular hydrogen can be comparable with the vibrational relaxation time because energy gaps between adjacent rotational states are as large as those between vibrational states. Therefore, for hydrogen, rotational nonequilibrium has to be coupled with vibrational nonequilibrium in numerical simulations of hypersonic flows.

Sharma derived the rotational relaxation times of molecular hydrogen for temperatures up to 5000 K by solving the master equations for ro–vibrational energy levels.[10] A quasi-classical-trajectory (QCT) method by Schwenke[11] is employed to obtain the ro–vibrational state-to-state transition rates. Their work is extended in the present work for the following reasons. First, the relaxation times considered up to 5000 K by Sharma are not sufficient to cover the flow regimes of outer planet entries. Second, because of the unconventional definition, their relaxation time rapidly decreases with the increase in temperature and ultimately becomes shorter than the average elastic collision time at temperatures over 5000 K. For these reasons, their results cannot be used directly in the conventional computational fluid dynamics (CFD). Moreover, the coupling phenomenon between rotational and vibrational modes was not discussed in detail. The authors consider that the knowledge of the coupling phenomena will help to develop the relaxation model for CFD.

The ultimate goal of this study is to establish a thermochemical model describing the internal energy relaxation for molecular hydrogen that is applicable to CFD simulations. Because the state-to-state rates used in Sharma's work were not available to the present authors, the state-to-state rates are recomputed by the QCT method using an existing code. The state-to-state rates so obtained are found to differ from Sharma's value by a simple factor. For the purpose of performing comparative calculations with Sharma, modification is made to the present values to bring the rates to approximately the same values as Sharma's. Some of the obtained rates are validated by the existing experimental data. Then the master equation for the ro–vibrational energy levels is solved using the obtained QCT state-to-state rates. The relaxation times appropriate to the Landau–Teller equation model are derived from the results.

II. Methods of Analysis

A. State-to-state Rate Coefficients

To obtain realistic state-to-state rate coefficients, the QCT calculations of H_2–H_2 bimolecular collisions are performed. The potential surface of the H_4 system is taken from a detailed analytical expression in Ref. 11, which is determined from the results of abinitio calculations. To be consistent, all of the discrete ro–vibrational energy levels are determined by solving the vibrational Schrödinger equation with the internuclear potential for the electronic ground state taken from Ref. 11, with a modification to take into account the molecular rotational motion corresponding to the rotational quantum number J. This approach yields the rotational energy levels of $J = 0$–38 and the vibrational energy levels of $v = 0$–14. The maximum numbers of the vibrational energy levels for each of the rotational energy levels are summarized in Table 1.

To compute the rate of $(J, v) \rightarrow (J', v')$ transition, the initial rotational and vibrational quantum number of the target molecule is set as (J, v). For the projectile molecule, the initial rotational and vibrational quantum numbers are given by statistical sampling of the Boltzmann distribution functions for the rotational and the vibrational temperature given in each computation. The initial kinetic energies of rotation and vibration are determined from the energy level of the corresponding quantum numbers. The initial phase angles of the rotational and vibrational motion and the direction of the angular momentum vector of both of the target and the projectile are given by appropriate random sampling. In this way, the initial state of the rotational and the vibrational motion of the target and the projectile are determined consistently. The relative velocity of collision is given by statistical sampling of the Boltzmann distribution function of the relative velocity at the translational temperature. The impact parameter b is given by statistical sampling within the maximum impact parameter $b_{\max}$, as $b = b_{\max}\sqrt{U}$. The initial distance between the two molecules is set to 10 Å. This value is large enough to have no influence on the result for the H_2–H_2 interaction in the temperature range of $1000 < T < 50{,}000$ K. On the same criterion, the calculation is terminated when the distance between the two molecules exceeds 12 Å after a collision. If the internuclear distance of a molecule exceeds 5 Å after a collision, the molecule in question is regarded to be dissociated.

Based on classical mechanics, the rotational and the vibrational motion of both the target and the projectile molecule are calculated in a time-marching fashion from the initial state described earlier. For the numerical procedures, the Lagrangian equations of motion for the four atoms are integrated in time by the fourth-order Runge–Kutta method. The final state of the internal modes of the target molecule is determined as the discrete level according to the final ro–vibrational energy after a collision. In this procedure, rotational transitions are allowed to occur between even or odd levels due to homonuclear nature of H_2. The continuous internal energy is discretized into the quantum levels in the following manner.[12,13]

Table 1 Maximum vibrational levels

J	$v_{\max}$	J	$v_{\max}$	J	$v_{\max}$	J	$v_{\max}$
0	14	10	12	20	8	30	3
1	14	11	12	21	8	31	3
2	14	12	11	22	7	32	2
3	14	13	11	23	7	33	2
4	14	14	11	24	6	34	1
5	14	15	10	25	6	35	1
6	13	16	10	26	5	36	0
7	13	17	9	27	5	37	0
8	13	18	9	28	4	38	0
9	12	19	9	29	4	——	——

From the final angular momentum about rotational motion, we chose the most probable two rotational quantum numbers, J and $J+2$. According to the final energy determined from the classical motion of atoms, four probable ro–vibrational quantal levels, (J, v_J) and (J, v_J+1) for J, and $(J+2, v_{J+2})$ and $(J+2, v_{J+2}+1)$ for $J+2$, are selected as candidates. Let us label these four candidates by 1, 2, 3, and 4, respectively. The probability for each of the candidate levels to be selected is defined by

$$P_i = \frac{1/|E_{\mathrm{rv}} - E_i|^n}{\sum_{i=1,4} 1/|E_{\mathrm{rv}} - E_i|^n} \tag{1}$$

where E_i is the ro–vibrational energy of ith candidate, and E_{rv} is the final ro–vibrational energy determined from the classical motion of atoms. In this study, n is taken to be 3 because it reproduces the experimental results most appropriately. According to these probabilities, the quantum level is determined in a statistical manner.

Finally, a set of the ro–vibrational state-to-state rates can be obtained by compiling the statistics of the final internal state of the target molecule after a large number of trial calculations of the bimolecular collision. The rate of transition from (J, v) to (J', v') is determined by

$$k_{J,v\to J',v'} = \sqrt{8kT/\pi\mu}\,\pi b_{\max}^2 N_{J,v\to J',v'}/N_{\mathrm{trial}} \tag{2}$$

After several preliminary calculations are tried, the minimum value for $b_{\max}$ is determined so that an accurate rate can be calculated efficiently.

B. Master Equations

In the present study, we consider the following heat bath problem. A hydrogen gas initially in the equilibrium state at $T_0 = T_{r0} = T_{v0}$ undergoes a sudden elevation of the translational temperature up to $T(>T_0)$. Rotational temperature T_r and vibrational temperature T_v increase due to relaxation of the internal energy until a thermal equilibrium among temperatures is established, while the translational temperature is kept unchanged.

Relaxation processes considered in the present study are the following collision-induced state-to-state transitions, state-specific dissociation, and state-specific recombination,

$$\mathrm{H_2}(J, v) + M \leftrightarrow \mathrm{H_2}(J', v') + M \tag{3}$$

$$\mathrm{H_2}(J, v) + M \leftrightarrow \mathrm{H} + \mathrm{H} + M \tag{4}$$

where $\mathrm{H_2}(J, v)$ stands for a molecular hydrogen in the ro–vibrational state (J, v), H is an atomic hydrogen, and M is a possible collision partner. Although M can be replaced by $\mathrm{H_2}(J, v)$ or H, we only consider $M = \mathrm{H_2}$ for approximation, because we are interested in the early phase of relaxation where collisions between molecules are more likely than between a molecule and an atom.

From the QCT analysis, we can obtain the rate coefficients for the ro–vibrational transition of Eq. (3) and for the dissociation of Eq. (4). Because the rate coefficients of recombination cannot be calculated in the QCT analysis, they are calculated by the detailed balance equations, using the state-specific dissociation rates obtained earlier. So that the detailed balancing relationship can be consistently satisfied between the upward and the downward ro–vibrational state-to-state transitions, the downward rate is recalculated from the corresponding upward rate. Here, we define the upward transition as a transition in which the ro–vibrational energy increases.

Time evolution of the number density of molecular hydrogen in the ro–vibrational state (J, v) due to Eqs. (3) and (4) is governed by the following master equations:

$$\frac{\mathrm{d}n_{J,v}}{\mathrm{d}t} = \left[\sum_{J'}\sum_{v'} k_{J',v'\to J,v}\, n_{J',v'} - \sum_{J'}\sum_{v'} k_{J,v\to J',v'}\, n_{J,v} - k_{J,v\to c}\, n_{J,v} + k_{c\to J,v}\, n_{\mathrm{H}} n_{\mathrm{H}} \right] n_{\mathrm{H_2}} \tag{5}$$

The master equation for the number density of atomic hydrogen is given by

$$\frac{\mathrm{d}n_{\mathrm{H}}}{\mathrm{d}t} = 2\sum_{J'}\sum_{v'} [k_{J',v'\to c} n_{J',v'} - k_{c\to J',v'} n_{\mathrm{H}} n_{\mathrm{H}}] n_{\mathrm{H_2}} \tag{6}$$

Equations (5) and (6) are normalized in the manner described in Ref. 14. By the introduction of the detailed balancing relationship between the upward and downward transitions,

$$k_{J,v\to J',v'}/k_{J',v'\to J,v} = n_{J',v'\mathrm{eq}}/n_{J,v\,\mathrm{eq}} \tag{7}$$

$$k_{J,v\to c}/k_{c\to J,v} = (n_{\mathrm{H\,eq}})^2 / n_{J',v'\mathrm{eq}} \tag{8}$$

Eqs. (5) and (6) are reduced to

$$\frac{\mathrm{d}\rho_{J,v}}{\mathrm{d}Z} = \sum_{J'}\sum_{v'} K_{J,v\to J',v'}[\rho_{J',v'} - \rho_{J,v}] + K_{J,v\to c}\left[\rho_{\mathrm{H}}^2 - \rho_{J,v}\right] \tag{9}$$

$$\frac{\mathrm{d}\rho_{\mathrm{H}}}{\mathrm{d}Z} = 2\sum_{J'}\sum_{v'} K_{J',v'\to c}\left[\rho_{J',v'} - \rho_{\mathrm{H}}^2\right]\frac{n_{J',v'\,\mathrm{eq}}}{n_{\mathrm{H\,eq}}} \tag{10}$$

The normalized nonequilibrium populations are defined by

$$\rho_{J,v} = n_{J,v}/n_{J,v\,\mathrm{eq}} \tag{11}$$

$$\rho_{\mathrm{H}} = n_{\mathrm{H}}/n_{\mathrm{H\,eq}} \tag{12}$$

The collision number is defined by the mean collision time as

$$Z = \frac{t}{t_c} = \frac{4}{\pi}\frac{16}{5}\frac{n_{\mathrm{H_2}} kT\Omega^{(2,2)}}{\sqrt{\pi mkT}}t \tag{13}$$

The collision integral $\Omega^{(2,2)}$ up to $T = 15{,}000$ K is taken from Ref. 15 and is extrapolated for higher temperature. The normalized rate coefficients for state-to-state transition and for state-specific dissociation are, respectively, given by

$$K_{J,v\to J',v'} = k_{J,v\to J'v'}/K_c \tag{14}$$

$$K_{J,v\to c} = k_{J,v\to c}/K_c \tag{15}$$

where the elastic collision rate is defined by

$$K_c = 1/t_c n_{\mathrm{H_2}} = (4/\pi)(16/5)\left(kT\Omega^{(2,2)}/\sqrt{\pi mkT}\right) \tag{16}$$

The normalized master equations (9) and (10) are integrated in time using $k_{J,v\to J'v'}$ and $k_{J,v\to c}$ obtained from the QCT results. The fourth-order Runge–Kutta method with adaptive step-size control (see Ref. 16) is employed for time integration.

C. Bulk Dissociation and Recombination Rate Coefficients

For collisional dissociation and recombination process for hydrogen molecules,

$$\mathrm{H_2} + M \leftrightarrow \mathrm{H} + \mathrm{H} + M \tag{17}$$

time evolution of the number density for molecular hydrogen can be written by

$$\frac{\mathrm{d}n_{\mathrm{H_2}}}{\mathrm{d}t} = -\left[k_d n_{\mathrm{H_2}} - k_r n_{\mathrm{H}} n_{\mathrm{H}}\right] n_{\mathrm{H_2}} \tag{18}$$

From Eq. (10), the time evolution of $n_{\mathrm{H_2}}$ is also given by

$$\frac{\mathrm{d}n_{\mathrm{H_2}}}{\mathrm{d}t} = -\frac{1}{2}\frac{\mathrm{d}n_{\mathrm{H}}}{\mathrm{d}t} = -\sum_{J'}\sum_{v'} [k_{J',v'\to c} n_{J',v'} - k_{c\to J',v} n_{\mathrm{H}} n_{\mathrm{H}}] n_{\mathrm{H_2}} \tag{19}$$

Comparing the first terms in the right-hand side of Eqs. (18) and (19) and considering the relationship of

$$n_{H_2} = \sum_J \sum_v n_{J,v}$$

we obtain the bulk dissociation rates as

$$k_d = \frac{\sum_J \sum_v k_{J,v\to c}\, n_{J,v}}{\sum_J \sum_v n_{J,v}} \tag{20}$$

The bulk recombination rate coefficients can be obtained by the following Saha equation:

$$k_d/k_r = (n_{H\,eq})^2 \big/ n_{H_2 eq} = K_{eq} \tag{21}$$

D. Vibrational and Rotational Relaxation Time

In the present analysis, the vibrational relaxation time is determined in terms of the bulk vibrational temperature defined from the average vibrational energy. The average vibrational energy per molecule is given by

$$e_{vib} = \frac{\sum_J \sum_v (e_{J,v} - e_{J,0})\, n_{J,v}}{\sum_J \sum_v n_{J,v}} \tag{22}$$

The bulk vibrational temperature is determined by solving the equation

$$e_{vib} = \frac{k\theta_v}{\exp(\theta_v/T_v) - 1} \tag{23}$$

where $\theta_v = [e_{0,1} - e_{0,0}]/k = 5946.7$ K. Provided that the vibrational energy relaxation follows the Landau–Teller equation

$$\frac{de_{vib}(T_v)}{dt} = \frac{e_{vib}(T) - e_{vib}(T_v)}{\tau} \tag{24}$$

the so-called e-folding relaxation time τ is determined as the time at which the vibrational energy satisfies the following relationship:

$$\frac{e_{vib}(T) - e_{vib}(T_v)}{e_{vib}(T) - e_{vib}(T_{v0})} = \frac{1}{e} \tag{25}$$

Using Eq. (25) as the criterion, we determine the vibrational relaxation time from the time evolution of the vibrational energy obtained by time integration of the master equations.

In the same manner, the rotational relaxation time is determined as the time when $(T - T_r)/(T - T_0) = 1/e$ is satisfied. The average rotational energy per molecule is given by

$$e_{rot} = \frac{\sum_J \sum_v e_{J,0} n_{J,v}}{\sum_J \sum_v n_{J,v}} \tag{26}$$

The bulk rotational temperature is determined by the relationship

$$T_r = e_{rot}/k \tag{27}$$

III. Test Conditions

The QCT calculations were carried out for the temperatures $T = T_r = T_v = 1000$, 3000, 5000, 10,000, and 50,000 K. The values of b_{max} used in the present study are 5.0, 4.5, 4.0, 3.5, and 3.5 Å for 1000, 3000, 5000, 10,000, and 50,000 K, respectively. Calculations were done for all of the possible initial ro–vibrational states, which amount to 350 in total. In each case of the initial ro–vibrational state, 5000 trajectories are calculated to obtain the state-to-state rates.

The master equations are integrated for five heat-bath temperatures of 1000, 3000, 5000, 10,000, and 50,000 K. The initial conditions are summarized in Table 2. The translational temperature is assumed to be constant at the heat-bath temperature throughout the integration. The conditions of cases 1, 5, and 6 are taken from Ref. 10 for the purpose of comparison. Effects of the initial rotational and vibrational temperature and the initial total number density on solutions are examined by varying their values. The normalized time interval for numerical integrations of Eqs. (9) and (10) is varied in the range between 10^{-10} and 0.5 according to the maximum increment of the variables during the time step.

Table 2 Initial conditions

Case	T, K	$T_{r0} = T_{v0}$, K	N_{H_2}, molecules
1	5,000	4,000	1.0×10^{23}
2	10,000	300	1.0×10^{23}
3	10,000	300	1.0×10^{18}
4	50,000	300	1.0×10^{18}
5	1,000	800	1.0×10^{23}
6	3,000	2,800	1.0×10^{23}
7	10,000	8,000	1.0×10^{23}
8	50,000	40,000	1.0×10^{23}

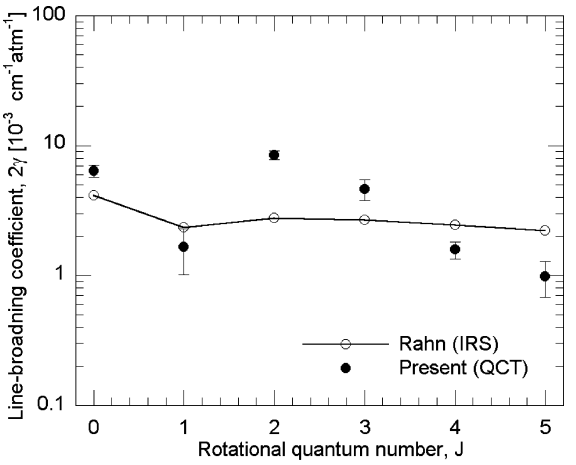

Fig. 1 Comparisons of the calculated line-broadening coefficients and experimental data of Rahn et al.,[17] $T = 1000$ K and $v = 1$.

IV. Results and Discussions

A. State-to-State Rate Coefficients

To validate the present QCT results, the total rotational transition rates are compared with the experimental data of the Raman Q-branch self-broadening coefficients of molecular hydrogen. In Ref. 17, Rahn et al. measured the broadening coefficients for $J = 0$–5. If the vibrational transitions are neglected, we can obtain the line-broadening coefficients by substituting the rotational state-to-state rates into the following equation[12,13]:

$$\gamma_J = 3.896 \times 10^{16} \sum_{J'} \frac{k_{J\to J'}}{T} \tag{28}$$

The present results for 1000 K are compared with the data of Rahn et al. in Fig. 1. The present results agree reasonably well with the experimental data. Error bars on the numerical results in Fig. 1 are given by the statistical standard deviations.

The vibrational transition rates obtained in the QCT analysis are compared in Fig. 2 with the experimental data of Audibert et al.[18] and Dove and Teitelbaum,[19] and with the past calculations done by Zenevich et al.[20] To obtain the $K_{10\to 00}$ rate, additional QCT calculations are carried out. In the calculations, the initial vibrational quantum number of the target molecule is fixed at $v = 1$ and that of the projectile at $v = 0$. The initial rotational quantum numbers of both molecules are given by statistical sampling. Even though the present rates are all larger than the experimental data of Dove et al., their values remain within the same order of magnitude, and the temperature dependence is the same as those of the experimental and analytical results.

From these comparisons, the present QCT rates are believed to be valid in the low-temperature range up to 3000 K. Unfortunately, no experimental data are available to validate the transition rates at higher temperatures.

Typical values of the state-to-state and the state-specific dissociation rate coefficients are compared with the results of Sharma[10] in Fig. 3a. The present rate coefficients are larger than Sharma's for the temperatures over 3000 K, although in good agreement for 1000 K.

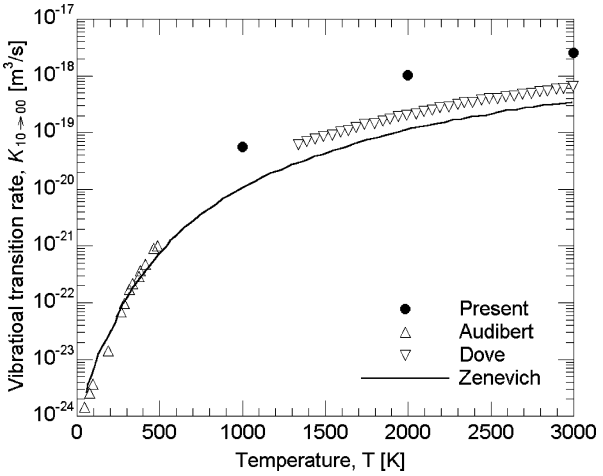

Fig. 2 Comparisons of calculated vibrational transition coefficients, experimental data of Audibert et al.,[18] Dove and Teitelbaum,[19] and semiclassical calculation of Zenevich et al.[20]

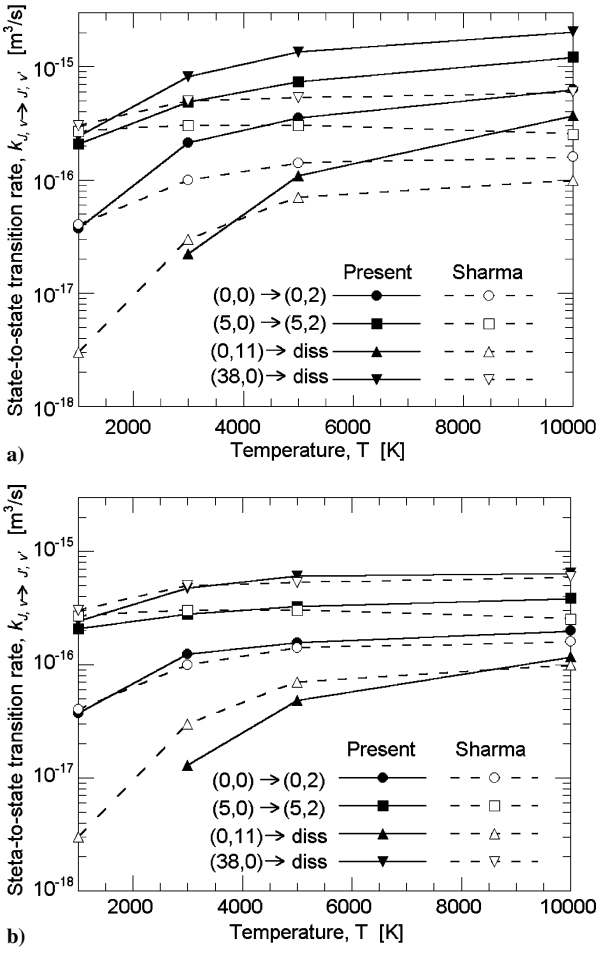

Fig. 3 Comparisons of state-to-state transition and dissociation rate coefficients: a) present uncorrected and Sharma's[10] rates and b) present corrected and Sharma's rates.

Note that, by introducing a simple correction factor, the rates approximately the same values as Sharma's can be obtained, as shown in Fig. 3b: The modified values are obtained by $k_{\rm cor} = k_{\rm org}/\sqrt{(T/1000)}$, where $k_{\rm org}$ and $k_{\rm cor}$ are the original and the modified values, respectively.

B. Recombination Rate Coefficients at Quasi Steady State

Evolution of the bulk rotational and the bulk vibrational temperatures for case 1 with the uncorrected state-to-state rate are shown in Fig. 4. The rotational and the vibrational temperatures stop increasing at the collision number of 1000 before reaching the final equilibrium temperature and keep almost constant temperature value of about 4800 K for a further 100,000 collisions. Such plateaus in temperature profiles are also seen in the calculated result for case 2 in Fig. 5. These are the so-called quasi steady state (QSS). Variation of initial number density of molecular hydrogen affects the period of QSS for this case, but not the temperature value at which QSS appears. The period of the QSS becomes long when the total number density is decreased in case 3 (Fig. 5). Variation of initial rotational and vibrational temperatures affects neither the period of nor the temperature value during QSS. In the calculations with the initial rotational and the vibrational temperatures of 2000 and 5000 K, QSS appears at the same temperature and lasts for the same collision numbers as case 2 (figures not shown). The variation of normalized population distribution for case 2 is shown in Fig. 6. The normalized population distribution is defined by $(n_{J,v}/n_{\rm H_2})/(n_{J,v}/n_{\rm H_2})_{\rm eq}$ in the present study. At the early phase of relaxation, high-energy levels approach the equilibrium population more quickly than the low-energy levels, as seen in the population distributions at $Z = 1$ and 10. However, at $Z = 500$ under QSS, the high-energy levels are underpopulated, whereas the lower levels are almost completely equilibrated. Such a population distribution remains unchanged until the rotational and the vibrational temperature start increasing again as shown in Fig. 5. This indicates that the incoming and the outgoing rate of population at an energy level (J, v) are almost balanced under QSS.

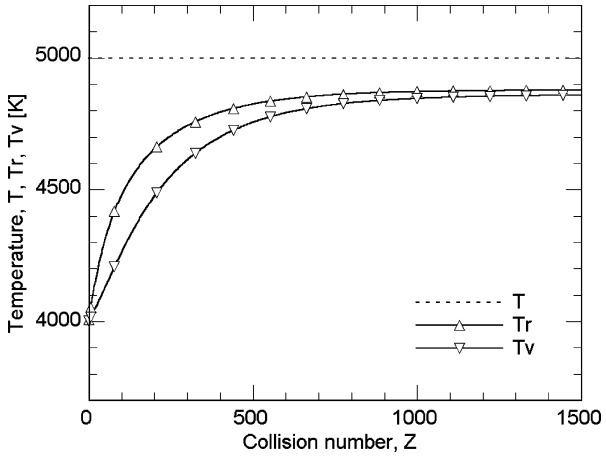

Fig. 4 Temperatures evolution in calculation for case1.

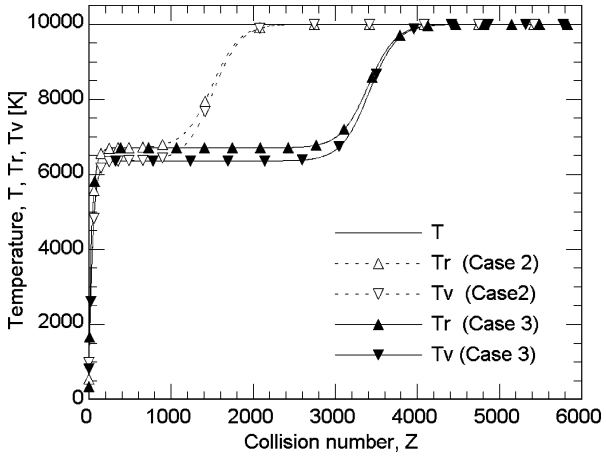

Fig. 5 Temperature evolution in calculation for cases 2 and 3.

The recombination rate coefficients under QSS are determined from the present results and compared with the existing studies. The bulk QSS recombination rate coefficients can be calculated by Eq. (20) when we know the number densities of each ro–vibrational energy levels, $n_{J,v}$, under QSS. Here, we examine two different

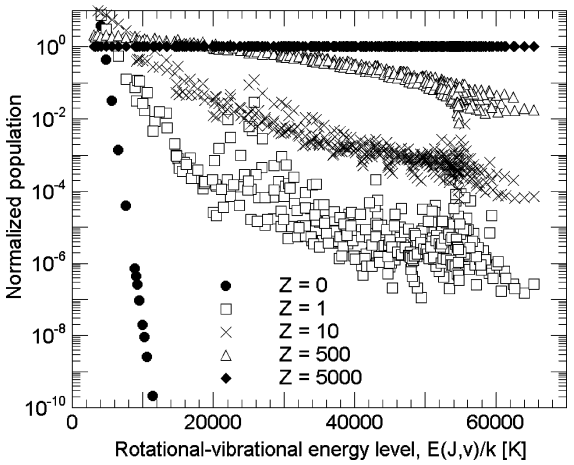

Fig. 6 Normalized population of the rotational–vibrational energy levels at various collision numbers for case 2.

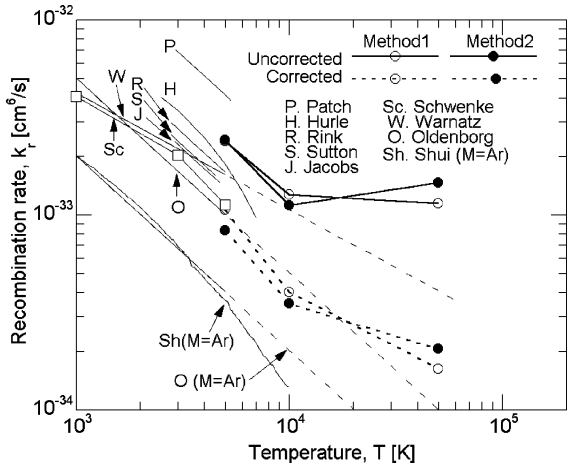

Fig. 7 QSS recombination rates.

methods to obtain the number densities under QSS. Method 1 is substituting the values of $n_{J,v}$ that are determined by solving equations (9) with setting the left-hand side to zero.[7,21] Method 2 is substituting the values of $n_{J,v}$ at the local time when the QSS condition is satisfied during the time integration of Eqs. (9) and (10). The corresponding conditions for calculations are cases 1, 3, and 4 in Table 2. As shown in Fig. 7, these two methods give the almost same values of recombination rates. In Fig. 7, the existing expressions for the recombination rate coefficients are displayed: the experimental expressions by Patch,[22] Hurle,[23] Rink,[24] Sutton,[25] and Jacobs et al.[26]; the theoretical results by Schwenke[27] and Shui et al.[28]; and the recommended expressions by Oldenborg et al.[29] and Warnatz.[30] Most of the experimental expressions are clustered between the present results with the uncorrected and the corrected state-to-state rates at 5000 K. When the uncertainties of the experimental expressions are considered, the both of uncorrected and corrected state-to-state rates give reasonable values of recombination rates at 5000 K. The slopes of the rates between 5000 and 10,000 K in the present results also agree well with the experimental expressions. However, for the temperatures over 10,000 K, the temperature dependency obtained by the uncorrected state-to-state rates shows a upward trend in contrast with the concave downward trend of Shui et al.[28] that are deduced from the modified phase-space theory. Although such a temperature dependency in also seen in the results with the corrected state-to-state rates, the calculated values agree reasonably with the extrapolated line of the recommended expression by Oldenborg et al.[29]

C. Ro–Vibrational Energy Loss due to Dissociation at QSS

Under the QSS condition, the dissociation of molecular hydrogen is likely to occur from higher ro–vibrational energy states as mentioned in the preceding section. In such a case, the bulk gas loses relatively large amount of internal energies. Therefore, it is necessary to consider such a coupling effect between internal energy relaxations and dissociation reaction when we calculate flows with nonequilibrium phenomenon. The amount of the ro–vibrational energy loss is given by[21]

$$E_{\text{rot}-\text{vib loss}} = \frac{\sum_J \sum_v e_{J,v}[k_{J,v\to c} n_{J,v} - k_{c\to J,v} n_{\text{H}} n_{\text{H}}] n_{\text{H}_2}}{-\,\mathrm{d}n_{\text{H}_2}/\mathrm{d}t} \tag{29}$$

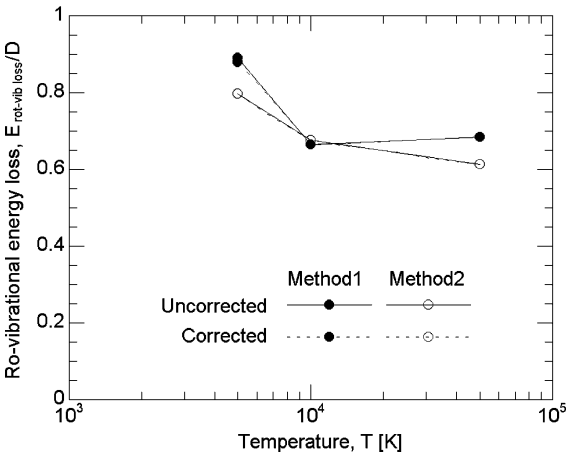

Fig. 8 Ro–vibrational energy loss due to dissociation, $D = 4.52$ eV = 52,454 K.

The calculated ro–vibrational energy losses due to dissociation at QSS are shown in Fig. 8. Methods 1 and 2 correspond to the methods obtaining the value of $n_{J,v}$, as mentioned in the preceding section. These two methods give the similar values of the ro–vibrational energy loss with the difference within 10%. Despite the discrepancy in the recombination rates, the uncorrected and the corrected state-to-state rates yield the same values of the ro–vibrational energy loss. From these results, it is found that the amount of energy loss at high temperatures above 10,000 K is about two-thirds of the dissociation energy.

D. Rotational and Vibrational Relaxation Time

The relaxation times are determined from the present results with the uncorrected and the corrected state-to-state transition rates. One of our interests is to know how many collisions are required for hydrogen molecules to dissociate behind a shock wave. Therefore, calculations in this subsection are simplified by ignoring dissociation reactions. The corresponding conditions for calculations are cases 1 and 5–8 in Table 2. Although there exist quantitative differences among the relaxation times given by using the corrected and the uncorrected rates, they show qualitatively the same tendencies of temperature dependence. Generally, the obtained values of the relaxation times calculated with the modified rates are larger than those obtained with the original rates by the factor of $\sqrt{(T/1000)}$ that is used in modification of the original rates.

The obtained vibrational relaxation times are presented in Fig. 9. In Fig. 9, the experimental data of Dove and Teitelbaum[19] are shown. Because the experimental data were given only in the temperature range 1350–3000 K, the extrapolated line is given in curves against the outside of the temperature range for the purpose of comparison. The relaxation parameter $p\tau_v$ that is the product of the partial pressure of molecular hydrogen, p, and the vibrational relaxation time τ_v shows an approximately linear relationship with $T^{-1/3}$. The calculated relaxation times using the uncorrected state-to-state rates approximately coincide with the extrapolated straight line of the experimental data of Dove and Teitelbaum, whereas those obtained with the corrected rates at the temperature of 3000 K ($T^{-1/3} = 0.0693$) is close to the experimental data. We could not obtain the vibrational relaxation time at 1000 K. This is because the number of QCT trials was not sufficient to obtain very small values of the rate coefficient at 1000 K.

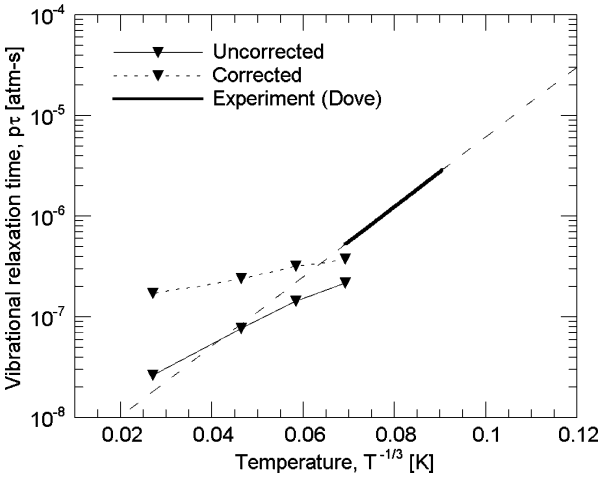

Fig. 9 Present vibrational relaxation time and experimental data of Dove and Teitelbaum.[19]

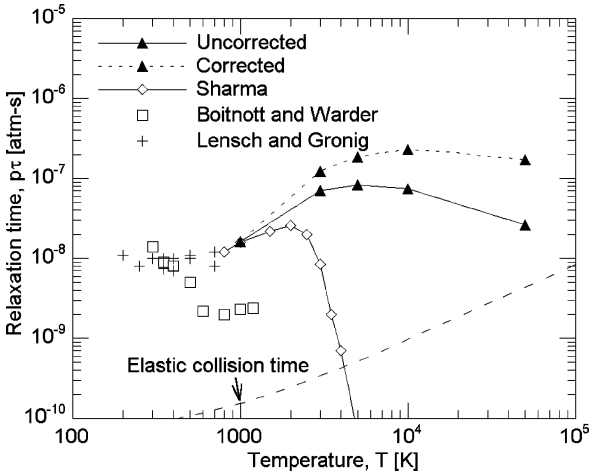

Fig. 10 Present rotational relaxation time, and calculationed results of Sharma,[10] and experimental data of Lensch and Gronig[31] and Boitnott and Warder.[32]

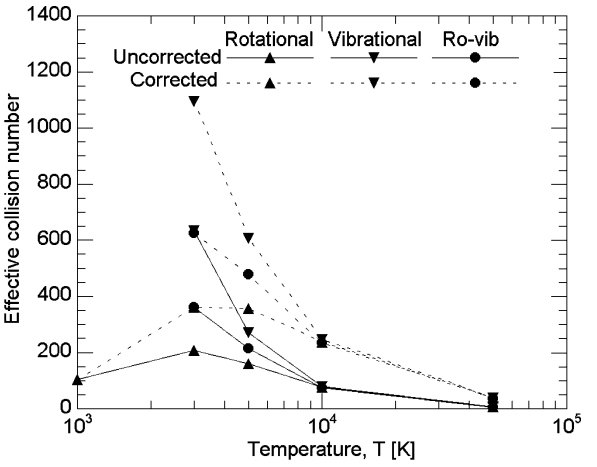

Fig. 11 Effective collision number for equilibration of rotational, vibrational, and ro–vibrational energy modes.

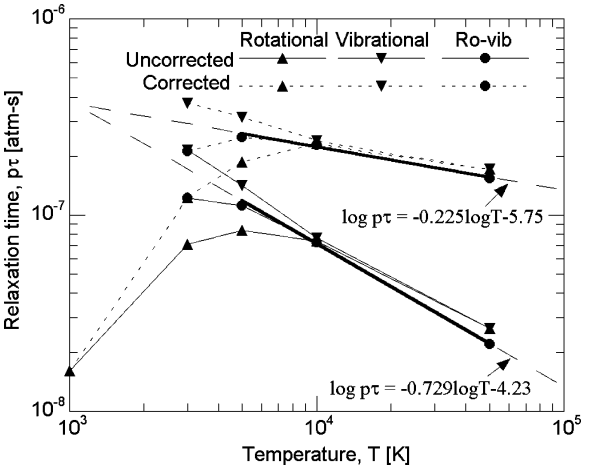

Fig. 12 Calculated rotational, vibrational, and ro–vibrational relaxation times and approximate expression of ro–vibrational relaxation time.

The obtained rotational relaxation times are presented in Fig. 10. The rotational relaxation times increase as the temperature increases up to 8000 K and then decrease as the temperature becomes higher. At 1000 K, all of the calculations give the same relaxation time as Sharma's and agreement with the experimental data with Lensch and Gronig[31] is satisfactory. Data of Boitnott and Warder[32] are also shown in Fig. 10. However, there is a large discrepancy of the relaxation times between the present and Sharma's calculation in the high-temperature range even if the state-to-state rates are taken to be the same as Sharma's rates. If the present values of $p\tau_r$ are multiplied by the mole fraction of molecules, they approach Sharma's values. Therefore, to use Sharma's values in CFD, they must be divided by the mole fraction of the molecules. As mentioned in the Introduction, the difference between the present and Sharma's results is attributed to the difference in the definition of the relaxation parameter $p\tau_r$.

Figure 11 shows the effective e-folding collision numbers required for equilibration of rotational and vibrational energy modes. With the uncorrected state-to-state rates, for the rotational energy mode, 200 collisions are required for reaching equilibrium at 3000 K and 6 collisions at 50,000 K. More than 600 collisions are required for the vibrational energy equilibration at 3000 K and 6 collisions at 50,000 K. With the corrected state-to-state rates, for the rotational energy mode, 360 collisions are required for reaching equilibrium at 3,000 K and 40 collisions at 50,000 K. The vibrational energy equilibration requires more than 1000 collisions at 3,000 K and 40 collisions at 50,000 K. The vibrational effective collision numbers coincide with the rotational ones at the temperatures over 10,000 K. This suggests that these two energy modes are strongly coupled to each other at high temperatures: The rotational and the vibrational energy modes are in an equilibrium state to each other. Therefore, the ro–vibrational energy mode, that is, the combination of rotational and vibrational energy modes,

$$e_{\text{rot-vib}} = \frac{\sum_J \sum_v e_{J,v} n_{J,v}}{\sum_J \sum_v n_{J,v}}$$

can be defined using the common temperature. The effective collision numbers of this ro–vibrational energy mode are also shown in Fig. 11. For this high-temperature range, the ro–vibrational relaxation times can be represented by the following expressions. For the uncorrected state-to-state rates,

$$\log p\tau = -0.729 \log T - 4.23 \text{ atm} \cdot \text{s} \tag{30}$$

For the corrected state-to-state rates,

$$\log p\tau = -0.225 \log T - 5.75 \text{ atm} \cdot \text{s} \tag{31}$$

These expressions are compared with the calculated values in the range of temperatures above 5000 K in Fig. 12. Because the temperature behind the shock wave is greater than 5000 K in all outer planet entries, the preceding expressions are believed to be sufficient in describing the influence of vibrational and rotational nonequilibrium therein.

V. Conclusions

The master equations with the QCT state-to-state rates are integrated to examine the behavior of rotational and vibrational energy modes of hydrogen molecules during relaxation, under the constant temperature conditions for temperatures from 1000 to 50,000 K. The relaxation times for rotational and vibrational modes are derived based on the Landau–Teller theory. The obtained vibrational relaxation times agree well with the existing experimental data at temperature below 3000 K. Coupled relaxations of rotational and vibrational energy modes are found for temperatures over 5000 K. Calculation of relaxation is performed using two sets of state-to-state transition rate coefficients, the present QCT rates or the values corrected to agree with the values by Sharma. The relaxation time τ of the coupled ro–vibrational mode for temperature above 5000 K is $\log p\tau = -0.729 \log T - 4.23$ using the uncorrected rates and $\log p\tau = -0.225 \log T - 5.75$ using the corrected rates.

Acknowledgments

This work has been supported by Research Fellow of the Japan Society for the Promotion of Science for Young Scientists. The authors would like to express their appreciation to Chul Park, Korean Advanced Institute of Science and Technology, Republic of Korea, for helpful comments and suggestions.

References

[1]Milos, F. S., "Galileo Probe Heat Shield Ablation Experiment," *Journal of Spacecraft and Rockets*, Vol. 31, No. 6, 1997, pp. 705–713.

[2]Park, C., "Heatshielding Problems of Planetary Entry, A Review," AIAA Paper 99-3415, June 1999.

[3]Matstuyama, S., "Numerical Study of Galileo Probe Entry Flowfield," Ph.D. Dissertation, Dept, of Aeronautic and Space Engineering, Tohoku Univ., Japan, Jan. 2004.

[4]Leibowitz., L. P., "Measurements of the Structure of an Ionizing Shock Wave in a Hydrogen–Helium Mixture," *Physics of Fluids*, Vol. 16, No. 1, 1973, pp. 59–68.

[5]Howe, J. T., "Hydrogen Ionization in the Shock Layer for Entry into the Outer Planets," *AIAA Journal*, Vol. 12, No. 6, 1974, pp. 875, 876.

[6]Bogdanoff, D. W., and Park, C., "Radiative Interaction Between Driver and Driven Gases in an Arc-Driven Shock Tube," *Shock Waves*, Vol. 12, No. 2, 2002, pp. 205–214.

[7]Park, C., *Nonequilibrium Hypersonic Aerothermodynamics*, Wiley, New York, 1989, Chaps. 3 and 5.

[8]Matsuzaki, R., "Effect of Free Electron and Rotational Coupling on Electron Temperature in Ionized Nonequilibrium Flow of Air," AIAA Paper 88-2669, June 1988.

[9]Park, C., "Assessment of Two-Temperature Kinetic Model for Ionizing Air," *Journal of Thermophysics and Heat Transfer*, Vol. 3, No. 3, 1989, pp. 233–244.

[10]Sharma, S. P., "Rotational Relaxation of Molecular Hydrogen at Moderate Temperatures," *Journal of Thermophysics and Heat Transfer*, Vol. 8, No. 1, 1994, pp. 35–39.

[11]Schwenke, D. W., "Calculations of Rate Constants for the Three-Body Recombination of H_2 in the Presence of H_2," *Journal of Chemical Physics*, Vol. 89, No. 4, 1988, pp. 2076–2091.

[12]Fujita, K., and Abe, T., "State-to-State Nonequilibrium Rotational Kinetics of Nitrogen Behind a Strong Shock Wave," AIAA Paper 2002-3217, June 2002.

[13]Fujita, K., and Abe, T., "Coupled Rotational–Vibration-Dissociation Kinetics of Nitrogen Using QCT Models," AIAA Paper 2003-3779, 2003.

[14]Park, C., "Rotational Relaxation of N_2 Behind a Strong Shock Wave," *Journal of Thermophysics and Heat Transfer*, Vol. 18, No. 4, 2004, pp. 527–533.

[15]Vanderslice, J. T., Stanley Weissman, Mason, E. A., and Fallon, R. J., "High-Temperature Transport Properties of Dissociation Hydrogen," *Physics of Fluids*, Vol. 5, No. 2, 1962, pp. 155–164.

[16]Press, W. H., Teukolsky, S. A., Vetterling, W. T., and Flannery, B. P., *Numerical Recipies in C*, Cambridge Univ. Press, London, 1992, Chap. 16.

[17]Rahn, L. A., Farrow, R. L., and Rosasco, G. J., "Measurement of the Self-Broadening of the H_2 Q(0-5) Raman Transition from 295 to 1000 K," *Physical Review A*, Vol. 42, No. 11, 1991, pp. 6075–6088.

[18]Audibert, M.-M., Vilaseca, J., and Lukasik, J., "Vibrational Relaxation of Ortho and Para-H2 in the Range 400–50 K," *Chemical Physics Letters*, Vol. 31, No. 6, 1975, pp. 232–236.

[19]Dove, J. E., and Teitelbaum, H., "The Vibrational Relaxation of H_2. I. Experimental Measurements of the Rate of Relaxation by H_2, He, Ne, Ar, and Kr," *Chemical Physics*, Vol. 6, No. 3, 1974, pp. 431–444.

[20]Zenevich, V. A., Billing, G. D., and Jolicard, G., "Vibrational–Rotational Energy Transfer in H_2–H_2 Collisions II. The Relative Roles of the Initial Rotational Excitation of Both Diatoms," *Chemical Physics Letters*, Vol. 312, No. 5-6, 1999, pp. 530–535.

[21]Sakamura, Y., "A Master Equation Study of Vibration–Dissociation Coupling in Shock Heated Oxygen Molecules," *Shock Waves*, Vol. 12, No. 5, 2003, pp. 361–373.

[22]Patch, R. W., "Shock-Tube Measurement of Dissociation Rates of Hydrogen," *Journal of Chemical Physics*, Vol. 36, No. 7, 1962, pp. 1919–1924.

[23]Hurle, I. R., "Measurements of Hydrogen-Atom Recombination Rates Behind Shock Waves," *Eleventh Symposium (International) on Combustion*, Combustion Inst., Pittsburgh, PA, 1967, pp. 827–836.

[24]Rink, J. P., "Shock Tube Determination of Dissociation Rates of Hydrogen," *Journal of Chemical Physics*, Vol. 36, No. 1, 1962, pp. 262–265.

[25]Sutton, E. A., "Measurement of the Dissociation Rates of Hydrogen and Deuterium," *Journal of Chemical Physics*, Vol. 36, No. 11, 1962, pp. 2923–2931.

[26]Jacobs, T. A., Giedt, R. R., and Cohen, N., "Kinetics of Hydrogen Halides in Shock Waves. II. A New Measurement of the Hydrogen Dissociation Rate," *Journal of Chemical Physics*, Vol. 47, No. 1, 1967, pp. 54–57.

[27]Schwenke, D. W., "A Theoretical Prediction of Hydrogen Molecule Dissociation–Recombination Rates Including an Accurate Treatment of Internal State Nonequilibrium Effects," *Journal of Chemical Physics*, Vol. 92, No. 12, 1990, pp. 7267–7282.

[28]Shui, V. H., Appleton, J. P., and Keck, J. C., "The Theree-Body Recombination and Dissociation of Diatomic Molecules: A Comparison Between Theory and Experiment," *Thirteenth Symposium (International) on Combustion*, Combustion Inst., Pittsburgh, PA, 1971, pp. 21–35.

[29]Oldenborg, R., Chinitz, W., Friendman, M., Jaffe, R., Jachimowski, C., Rabinowitz, M., and Schott, G., "Status Report of the Rate Constant Committee, NASP High Speed Propulsion Technology Team," Dec. 1989.

[30]Warnatz, J., "Rate Coefficients in the C/H/O System," *Combustion Chemistry*, Springer-Verlag, New York, 1984, Chap. 5.

[31]Lench, G., and Gronig, H., "Experimental Determination of Rotational Relaxation in Molecular Hydrogen and Deuterium," *Proceedings of the Eleventh International Symposium on Shock Tubes and Waves*, edited by B. Ahlborn, A. Hertzberg, and D. Russell, Univ. of Washington Press, Seattle, WA, 1977, pp. 132–139.

[32]Boitnott, C. A., and Warder, R. C., "Shock-Tube Measurements of Rotational Relaxation in Hydrogen," *Physics of Fluids*, Vol. 14, No. 11, 1974, pp. 2312–2316.